J Intell Robot Syst (2015) 78:21–32
DOI 10.1007/s10846-014-0055-4

On the Control of Human-Robot Bi-Manual Manipulation

Stephen Warren · Panagiotis Artemiadis

Received: 13 December 2013 / Accepted: 17 March 2014 / Published online: 17 April 2014

Abstract As robots begin to permeate the everyday human workspace to collaborate in innumerable and varied tasks, the robotic structure must adhere and replicate human-like gestures for effective interaction. Whether rehabilitation or augmentation, upper arm human-robot interaction is some of the most prevalent and investigated forms of collaboration. However, currently robotic control schemes fail to capture the true intricacies of anthropomorphic motion and intent during simple bi-manual manipulation tasks. This paper focuses on the introduction of bio-inspired control schemes for robot manipulators that coordinate with humans during dual arm object manipulation. Using experimental data captured from human subjects performing a variety of every-day bi-manual life tasks, we propose a bio-inspired controller for a robot arm, that is able to learn human inter- and intra-arm coordination during those tasks. Using dimensionality reduction techniques to make comprehensible the linear correlations of both arms in joint space we fit and utilize potential fields that attract the robot to human-like configurations. This method is then tested using real experimental data across multiple bi-manual tasks with a comparison made between the bio-inspired and traditional inverse kinematic controllers. Using a robotic kinematic chain identical to the human arm, models are evaluated for anthropomorphic configurations.

Keywords Anthropomorphism · Inverse kinematics · Human-robot cooperation · Bi-manual manipulation · Potential fields

S. Warren · P. Artemiadis (✉)
Human-Oriented Robotics and Control Lab,
School for Engineering of Matter, Transport and Energy,
Arizona State University, Tempe, AZ 85287, USA
e-mail: panagiotis.artemiadis@asu.edu

S. Warren
e-mail: swwarren@asu.edu

1 Introduction

During the last decade, there has been an increasing demand for robots that can interact, communicate and collaborate with humans. Robots have moved inside human's leaving and working environment, therefore their behavior must shift from purely robotic to human-like. Application fields ranging from service robotics (assistive devices, entertainment robots, augmentation robots) to therapeutic devices (orthotics, prosthetics, rehabilitation robots) require human-likeness in robot movements and efficient human-robot collaboration, in order to achieve seamless robot integration in the human environment. Robots have to move and act in environments designed for humans, and more importantly use tools for executing tasks designed for humans.

Robot manipulation is a well studied field that has seen remarkable developments in the last 30 years [1, 11, 18, 33]. Moreover, dual-arm robot manipulation has been widely investigated in the last decade [4–6, 16, 19, 26, 29, 30, 34, 35, 42, 44]. Nevertheless, it still belongs to the most demanding challenges in robotics. Most importantly, this challenge gains more interest if robots are to become useful in common household settings which are tailored for human arms and hands.

Interaction and collaboration with humans requires human-like behavior from the robot side. Such behavior will allow the human subject to be able to understand robot's intentions, correlate characteristics (e.g. robot configuration) with task execution, and seamlessly collaborate with the robot. For this reason past research has attempted to define laws for biomimetic trajectory planning and robot inverse kinematics [28]. Approaches for mimicking the human arm movements have been proposed [8] for everyday life tasks (e.g. drawing, handwriting). There have been also efforts to generate human-like motion by imitating human arm motion as closely as possible. In [22], a method to convert the captured marker data of human arm motions to robot motion using an optimization scheme is proposed. The position and orientation of the human hand, along with the orientation of the upper arm, were imitated by a humanoid robot arm. However, this method was not able to generate human like motions, given a desired three dimensional (3D) position for the robot end-effector. Similarly, most of the previous works on biomimetic motion generation for robots are based on minimizing posture difference between the robot and the human arm, using a specific recorded data set [27]. Therefore, the robot configurations are exclusively based on the recorded data set. In this way, the method can not generate new human-like motion. The latter is a major limitation for the kinematic control of anthropomorphic robot arms and humanoids, because the range of possible configurations is limited to the ones recorded from humans.

In order to model motion principles of human arm movements, cost functions have been also used in the past [10, 14, 41]. Hidden Markov Models (HMM) have been used for modeling arm motion towards robot imitation [7, 23, 24, 36, 38], as well as other unsupervised learning techniques [13, 17, 40], however most of the works are based on cost functions and optimization techniques that drive the robots based on a finite recorded set, while the models are unable to generalize. Finally, a partitioning of the human-like motion generation problem has been proposed in the past [3]. The upper arm joint values are first calculated for positioning the robot elbow, and then using that, the rest of the joints are evaluated. Such an approach can not be easily applied to robots having a kinematic structure different from that of the human upper limb though.

Although some of the previous studies have investigated the human arm motion during bi-manual tasks, inter-arm coordination has not been adequately understood. From the neurophysiology point of view, there are many studies that provide evidence that bi-manual tasks are governed by coordination patterns encoded in neural level [9, 12, 37, 39, 43]. However, a kinematic coordination model for bi-manual tasks is still to be defined.

In this paper we focus on the inter-arm (between the two arms), as well as the intra-arm (within one arm) joint coordination during bi-manual tasks involving collaboration of the two arms. More specifically, we model this coordination for a wide variety of everyday life tasks. Then we use this model for defining bio-inspired controllers for robots collaborating with humans. Using data captured from human subjects performing a variety of every-day life tasks employing their two arms, we propose a bio-inspired controller for a robot arm. This controller is able to learn human inter- and intra-arm coordination during those tasks. We embed human arm coordination in low-dimension manifolds, and build potential fields that attract the robot to human-like configurations. The method is tested using a simulated robot arm that is identical in structure to the human arm. A preliminary evaluation of the approach is also carried out using an anthropomorphic robot arm in bi-manual manipulation task with a human subject.

2 Data Processing and Analysis

In order to track the motion of the upper limbs, we choose to use the joint angles of the shoulder, elbow and wrist. For doing so, we need to compute the center of rotation of those joints (see Fig. 1). We compute the centers of rotation using markers on the rigid bodies of upper arm, forearm and palm respectively. However, there are cases where some of the

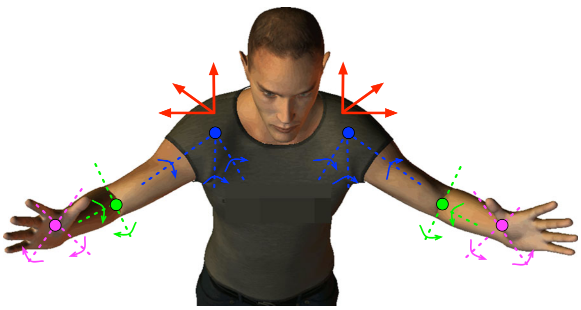

Fig. 1 Axes of modeled degrees of freedom and centers of rotations of the two arms

markers placed on those rigid bodies are obstructed from the camera's view. To combat this issue, a marker estimation process was created. It relied on the fact that each element of the position suit created, comprised of a rigid body, and the markers attached to this body would not shift with respect to each other. Therefore by capturing one or two frames from the data which had either all, or through both frames, a combination of all markers of the rigid body, we can build all the markers' inter-relationships. These relationships can be used to estimate a missing marker provided other markers from the same body are visible.

2.1 Biological Joint Centers and Calibration

The centers of rotation of the rigid bodies upper arm, forearm and palm, coincide with the biological joint centers shoulder, elbow and wrist respectively [15]. We used a calibration experiment, which required the human subject to attempt to move all joints simultaneously while capturing the position sensor data from the suit of markers. Then using a least squares method we were able to estimate the position of the biological centers with respect to the rigid body that precedes the kinematic chain of the arm. For example, we were able to estimate the center of rotation of the forearm (i.e. the elbow joint), with respect to the upper arm rigid body. Once these points are computed, they are projected into the base frame of reference located on the humans shoulder. Having the 3-dimensional (3D) position of the wrist and elbow, as well at the 3D position and orientation of the rigid body of the palm, we are able to analytically give a unique solution to the inverse kinematic problem, and therefore compute the

Table 1 Arm model D-H parameters

i	α_i	a_i	d_i	θ_i
1	90°	0	0	q_1
2	90°	0	0	$q_2 + 90°$
3	90°	0	L_1	$q_3 + 90°$
4	90°	0	0	$q_4 + 180°$
5	90°	0	L_2	$q_5 + 180°$
6	90°	0	0	$q_6 + 90°$
7	90°	L_3	0	$q_7 + 180°$

7 joint angles of the upper limb [31]. The Denavit-Hartenberg (DH) parameters of the kinematic model of the arm that we used are listed in Table 1, where L_1, L_2, L_3 are the length of the upper arm, forearm and palm respectively.[1]

2.2 Subjects and Task Protocol

For human motion experimental observation, 5 subjects in total were used. The subjects were four male, one female, with ages ranging from early to late 20s. There was a mixture of both self described right and left handedness in the test group. The experiments in bi-manual manipulation varied to encompass many types of manipulation coupling of the arms and tasks. The principal tasks were defined by a constant contact between the subject's hands and the object such as: cleaning dishes, removing and replacing a jar lid, stacking blocks, two handed pick and place, and many more. In contrast to the rigid coupling of the hands to the object, many tasks were chosen which still involved bi-manual manipulation but with greater freedoms for the subject to chose the configuration and path taken during the task. Some of the tasks were: tying shoe knots, fork and knife use while eating, using tools for mechanism assembly, placing and removing tape stuck on an object, and more. In total 15 tasks were selected and repeated three times each during the observation process. The reasoning behind the selection of tasks was to ensure both arms would be required for task completion but varied enough to show complex, non-repetitive, movements during the manipulation process.

[1]Offsets in θ_i are used for having the arm at rest position (pointing down) when $q_i = 0, i = 1, \ldots 7$.

3 Methods and Procedure

The idea of cost function minimization has been prevalent in robotic control since its inception. By penalizing the controller for unwanted manipulated variable moves or controlled variable locations, the designer may shape the profile and final output. For the robotic kinematic structure in collaboration with human users, the proposed solutions must satisfy two necessary constraints: the desired end-effector position and orientation to interact, but also the mimicry of common human configuration. Only when consideration for both is implemented in the solution will the human counterpart understand both the interactive approach and intention of the robotic device. The initial constraint can be solved easily through common manipulators with sufficient degrees of freedom. The second presents the challenge of quantifying an abstraction in anthropomorphism.

In order to achieve the desired anthropomorphic configurations during human-robotic collaborative tasks a method to shape the iterative inverse kinematic solution was devised. Potential minimization was selected due to its ability to provide simple quantification of success and robust functional description. The initial step for creating the governing cost or potential field is the experimental observation and statistical analysis during bi-manual manipulation as seen in the previous sections. However, the raw joint angle data represents a daunting task for functional analysis due to it's high order dimensionality and extreme non-linearities. In order transform the large dataset into a intelligible format statistical processing techniques were applied to reduce the data dimensionality through linear correlation. Once the data had been processed and molded into manageable form it could be functionally fitted through probability analysis from low order mixture models. These models would describe the full potential fields in a continuous form which allows for driving forces through vector gradients. The final step in the methodology is to apply these driving forces in the common inverse kinematic solution in order to achieve the overall goal of a bio-inspired control strategy. The methodology is summarized in Fig. 2. The following sections detail each step in the method proposed and detail pertinent modifications to common techniques when necessary.

3.1 Dimensionality Reduction and Inference

The kinematic relationships present in joint space during human bi-manual tasks are difficult to extract due to the large dataset dimensionality. For the full two arm human model a total of 14 separate and distinct joint angles were observed. Let

$$\mathbf{Q} = \left[\mathbf{q_1}\ \mathbf{q_2}\ \dots\ \mathbf{q_{14}}\right] \tag{1}$$

represent the $k \times 14$ matrix for the data set for all k observations of the 14 joint angles during experimentation. The observation matrix $\mathbf{Q}$ can also be grouped as $\mathbf{q_R}$ which represents the right arm joint angles in columns one through seven ($\mathbf{q_1}$-$\mathbf{q_7}$) of $\mathbf{Q}$ and similarly $\mathbf{q_L}$ as left arm joints ($\mathbf{q_8}$-$\mathbf{q_{14}}$) respectively. To obtain a reduced order, tangible model we use Principal Component Analysis (PCA) [20]. From the initial raw joint angle data the correlation matrix was computed on the zero-mean variance set from $\mathbf{Q}$. The PCA was then applied to the correlation matrix to examine the dual arm relationships in a lower dimensional form. After the deletion of non-contributing dimensions from the joint dataset, n dimensions are retained to describe a satisfactory variance description close to the original data. This transform is shown as

$$\sigma_{LR} = \mathbf{WQ} \tag{2}$$

where σ_{LR} is a n-dimensional vector to describe the dual arm variability, W is the $n \times 14$ matrix with columns of n principal eigenvectors computed through the PCA. Similarly σ_L and σ_R can be defined by selecting the columns of W to extract the appropriate components, for describing inter-arm coordination, from the joint observations: $\sigma_L = \mathbf{W_L q_L}$ a low-dimensional representation of the human left arm configuration.

The choice of components kept, for both dual arm and intra arm observation, were selected as to maximize the variance explanation while discarding as many components as possible. This was performed so that not only could the density functions be visualized but also the computational effort in the controller be reduced as it is a function of the retained principal components. Figure 3 shows three subject's left

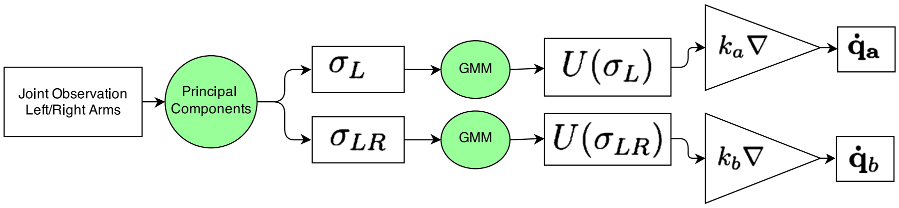

Fig. 2 Procedure overview: from joint observation to the creation of a lower dimensional space(σ). Utilizing Guassian mixture models to build PDFs and in turn potential functions U. Then by taking the gradient of the potential functions return joint velocities $\dot{q}$

arm joint variance explanation as a function of the retained components. No absolute method guarantees appropriate explanation percentage so the number was selected from visual inspection on convergence. In the case of left arm component retention, four were selected explaining around 85 % of original variance. For the dual arm (left-right) data it was found that a total of 8 dimensions could describe from 80 to 90 % variability across subjects. For more details of the application of the PCA in motion data the reader should refer to [2].

3.2 Characterization of Inter- and Intra-arm Coordination

The correlation among joints of the same arm, as well as across arms, is shown in the correlation matrix in Fig. 4. As it can be seen, many joints are correlated with each other, and correlations are evident across arms as well. Using the PCA method from above the low dimensional data for both dual arm σ_{LR} and single arm σ_L coordination lends itself to statistical analysis. Examining the configuration frequency of

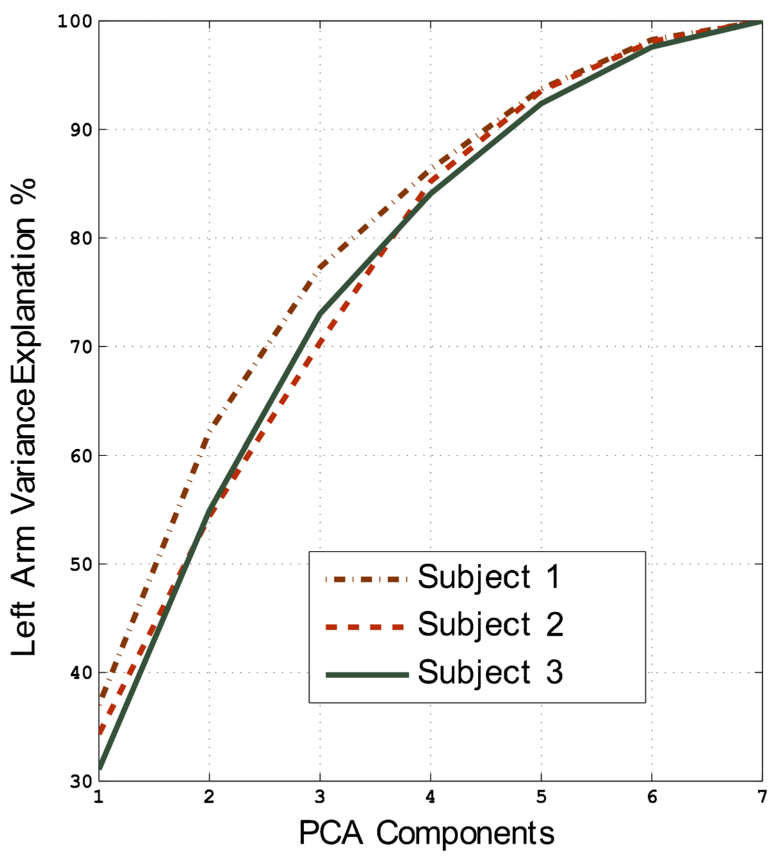

Fig. 3 Variance explanation VS. component selection for left arm $\mathbf{Q}_L$ observations on three subjects

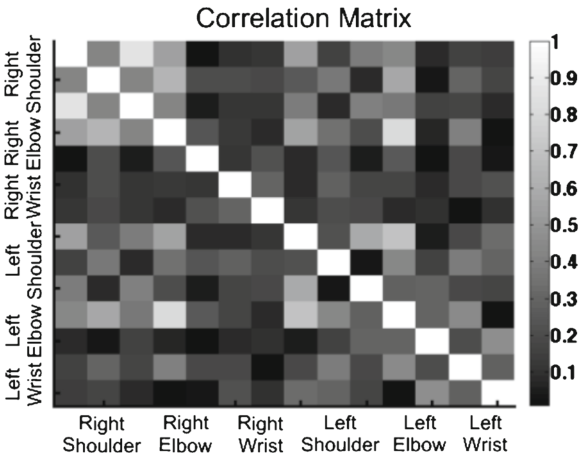

Fig. 4 Correlation matrix across all joints of both arms. Data from one representative subject are used

the human arm allows the construction of probability density functions (PDF). The dual arm correlation function for the left arm is described simplistically from:

$$P(\sigma_L|\sigma_R) = \frac{P(\sigma_L \cap \sigma_R)}{P(\sigma_R)}, \tag{3}$$

which states that the probability of a left arm joint configuration given a right arm configuration σ_R is given by the joint probability for both arms. Equation (3) represents the inter-arm coordination density field while the intra arm $P(\sigma_L)$ holds only the information of internal configuration likeliness. For visual representation only, Fig. 5 shows the PDFs which describe the two-dimensional representation of intra-arm coordination across all performed tasks for three subjects. These PDFs were fitted using experimental data across all trials for a given subject. To find the functional description of the PDFs for both the inter and intra-arm coordination the method of Gaussian Mixture Model (GMM) [25, 32] was utilized. This allowed for a continuous representation of the low dimensional dataset to allow for further manipulation, e.g. differentiation.

3.3 Potential Fields Through Probability Analysis

Driving a robot arm to configurations that were frequently observed in the human experiments would mean that we need to command the robot arm with a set of joint angles that lie on the region of high-probability of the PDF defined above. In order to do that, we transformed the probability density functions $f(\sigma)$ to potential fields $U(\sigma)$, where:

$$U(\sigma) = -f(\sigma) + f_{\max}(\sigma) \tag{4}$$

where $f_{\max}(\sigma)$ is the global maximum of the PDF. Potential fields have been used in robotics for a variety of reasons, especially in obstacle avoidance cases [21]. Here they are used to drive the robot configurations to regions that were observed in the human experiments. The way this is done is explained in the next sections.

3.4 Robot Inverse Kinematics

The main goal in controlling the robot to collaborate with the human is not only to drive the end-effector of the robot to a specific pose $\mathbf{x_d}$, but also impose a configuration $\mathbf{q_L}$ that will be anthropomorphic, or in other words, obey the inter- and intra-arm coordination of the human. For this reason, we choose to make use of the robot arm redundancy and solve the inverse kinematics iteratively using the block diagram described in Fig. 6. The robot arm angular velocity vector is given by

$$\dot{\mathbf{q}}_\mathbf{R} = \mathbf{J}_\mathbf{A}^{\dagger}\mathbf{K}\mathbf{e} + \left(\mathbf{I} - \mathbf{J}_\mathbf{A}^{\dagger}\mathbf{J}_\mathbf{A}\right)\dot{\mathbf{q}}_\mathbf{a} + \left(\mathbf{I} - \mathbf{J}_\mathbf{A}^{\dagger}\mathbf{J}_\mathbf{A}\right)\dot{\mathbf{q}}_\mathbf{b} \tag{5}$$

where $\mathbf{J_A}$ is the analytic Jacobian of the robot arm, $\mathbf{J}_\mathbf{A}^{\dagger}$ its pseudoinverse, $\mathbf{K}$ is a diagonal 7×7 gain matrix, $\mathbf{e} = \mathbf{x_d} - \mathbf{x}$ is the pose error between the desired pose $\mathbf{x_d}$ and the current one $\mathbf{x}$. The terms $\dot{\mathbf{q}}_\mathbf{a}$, $\dot{\mathbf{q}}_\mathbf{b}$ will cause *internal motion* of the robot arm, i.e. joint motion that would not affect the robot end-effector pose. This is due to the fact that they are multiplied with $\left(\mathbf{I} - \mathbf{J}_\mathbf{A}^{\dagger}\mathbf{J}_\mathbf{A}\right)$ that will project the motion to the null space of the robot Jacobian [31]. These terms are going to be used for imposing anthropomorphic characteristics based on the inter- and intra-arm coordination modeled using the PDFs defined above. It must be noted that for simplicity we assume that the robot arm has the same kinematics with the human arm it is replacing, and that the robot arm replaces the left human arm and collaborates with the right human arm.

Fig. 5 Probability density functions, projected in a two-dimensional space computed using the PCA for single (inter-arm) σ_L coordination across three subjects

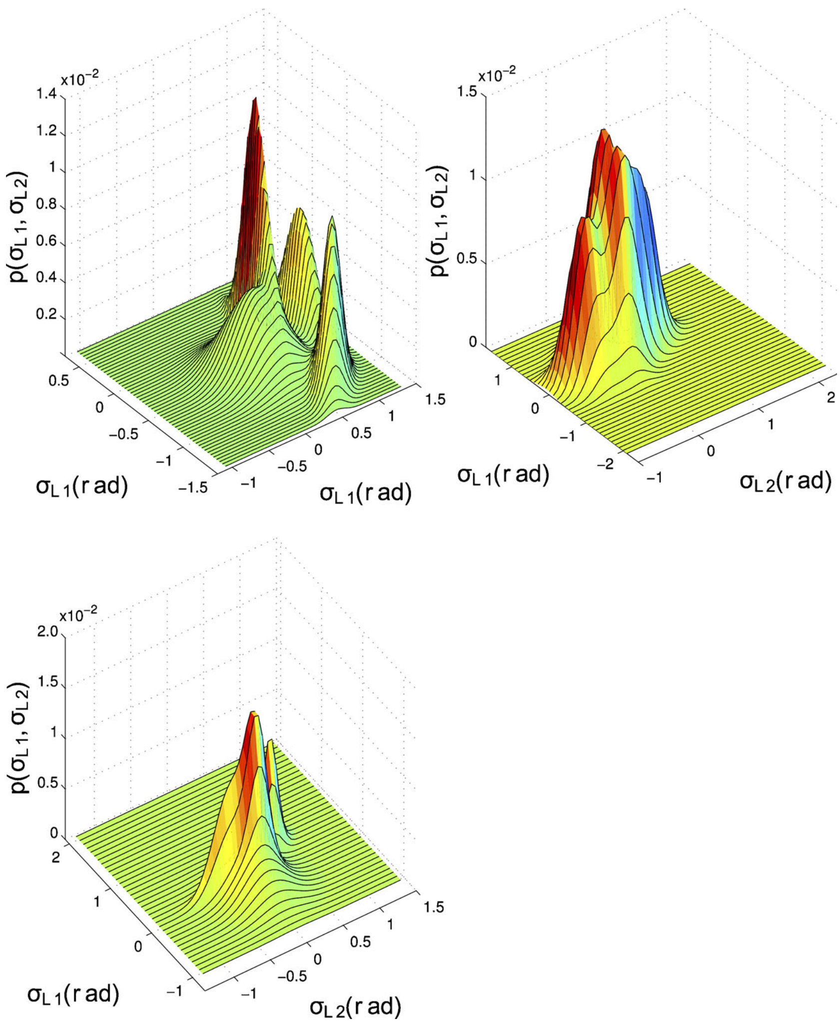

Both $\dot{\mathbf{q}}_\mathbf{a}$ and $\dot{\mathbf{q}}_\mathbf{b}$ terms are computed using the potential fields $U_L(\sigma_L)$ and $U_{LR}(\sigma_{LR})$. The potential fields are computed using Eq. 4 for the PDFs describing arm coordination respectively.

In order to capture the intra-arm (right arm) and inter-arm (right and left arms) coordination characteristics of the human, the robot is controlled using Eq. 5, where the terms $\dot{\mathbf{q}}_\mathbf{a}$ and $\dot{\mathbf{q}}_\mathbf{b}$ are given by:

$$\dot{\mathbf{q}}_\mathbf{a} = -k_a \nabla U_L(\sigma_L), \quad \dot{\mathbf{q}}_b = -k_b \nabla U_{LR}(\sigma_{LR}) \tag{6}$$

where k_a, k_b are positive gains. Equation (6) makes use of the robot redundancy in order to drive the robot arm to configuration that not only resemble the replaced left arm ($\dot{\mathbf{q}}_\mathbf{a}$ term), but also coordinate with the right human arm for bi-manual tasks ($\dot{\mathbf{q}}_\mathbf{b}$ term).

The novelty of the additional joint velocities is considering this extra input of the right arm configuration for the joint velocities. In both the internal and external functions which output additional joint velocities several issues arise when the current location in σ space is in either a point of almost no probability i.e. $P(\sigma) \simeq 0$ or near an area of minimum potential. In the first case

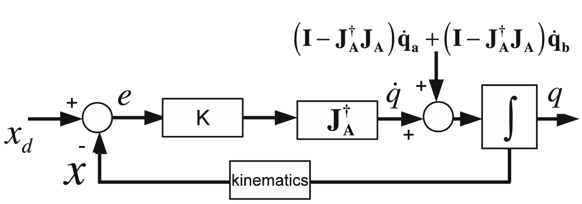

Fig. 6 Block diagram for iterative inverse kinematics using the pseudo-inverse Jacobian method and additional null space terms

the gradient terms have virtually no output as the gradient of the density functions (6) with outlier inputs is minuscule. The other case is when the joint configurations are near an ideal position in σ space, meaning they are close to a point of zero potential. This causes the gradients terms to become so large that overshoot and oscillation around a minimum point is inevitable. Therefore the gain term k_a and k_b in Eq. 6 must: over amplify in cases of low probability to have noticeable joint velocity contribution, and dampen when gradient terms would output high velocities. These conflicting conditions were combated by having the gain a function of the probability from the applicable density function as:

$$k = \frac{C}{P(\sigma)} \tag{7}$$

With k representing terms k_a or k_b and C being a constant gain multiplier. Another issue facing the final result of the inverse kinematic solution is θ_4, elbow flexion-extension, has no mapping onto the null space of $\left(\mathbf{I} - \mathbf{J}_\mathbf{A}^\dagger \mathbf{J}_\mathbf{A}\right)$. So an artificial perturbation term, for the elbow joint velocities, was included into the inverse kinematic controller (5). Using these modifications along with the standard inverse kinematic control led to the realization of a bio-inspired control strategy for the robotic manipulator.

4 Results and Discussion

Initially we tested whether the null space terms and the formulation of the potential fields could drive the robot arm to anthropomorphic configurations, that would coincide with local minima of the potential functions. For this reason, we started the robot from 3 distinct configurations, represented them in the low-dimensional space σ_L, and observed how the term $\dot{\mathbf{q}}_\mathbf{a}$ resulted to robot motion in the null space. Figure 7 shows the path of the robot in those 3 cases, where it is shown that the robot was successfully reconfigured in joint space to regions of low potential, therefore high probability based on the human experimental data.

The proposed inverse kinematic method was tested alongside the traditional, error only, inverse kinematic (IVK) solution. The controller was given information on the right arm joint configuration and end effector pose for the left arm from experimental data in

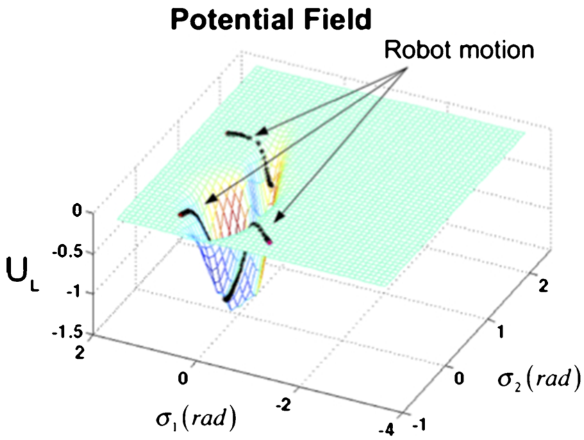

Fig. 7 Robot motion in the null space where robot arm is re-configured to meet anthropomorphic configurations. Representation in the low-dimensional space, using the potential field. Three cases with different initial conditions are shown

bi-manual object manipulation. The human joint comparison data was from a subject not used in building the potential function. The controllers were tested over a 2 second span during a bi-manual manipulation experiment. The results are shown in Fig. 8. This figure demonstrates, seen from the mean squared error of all joint angles, that the bio-inspired controller, without information on: joint limits, singularity, etc, outperformed the traditional pseudo-inverse Jacobian method for solving the robot inverse kinematics. It also demonstrates the bio-inspired controller's ability to drive the arm configuration to mimic the human one whereas the traditional controller has a constant offset. To examine the average error in both controllers several hundred trials were run to compare the final joint difference between the human data and that of the final configuration for the bio-inspired and traditional controller. As seen in Fig. 9 the proposed controller outperforms the traditional one substantially.

However, it must be noted that the goal of the proposed method is not to always drive the robot arm to specific configurations that were observed during the human motion data collection. In fact, our main goal is to create a method that would guarantee anthropomorphism in the robot arm motion, and would be able to generalize to motion not seen during the *training* phase with the human subject. Using the proposed potential field formulation, we drive the robot arm to

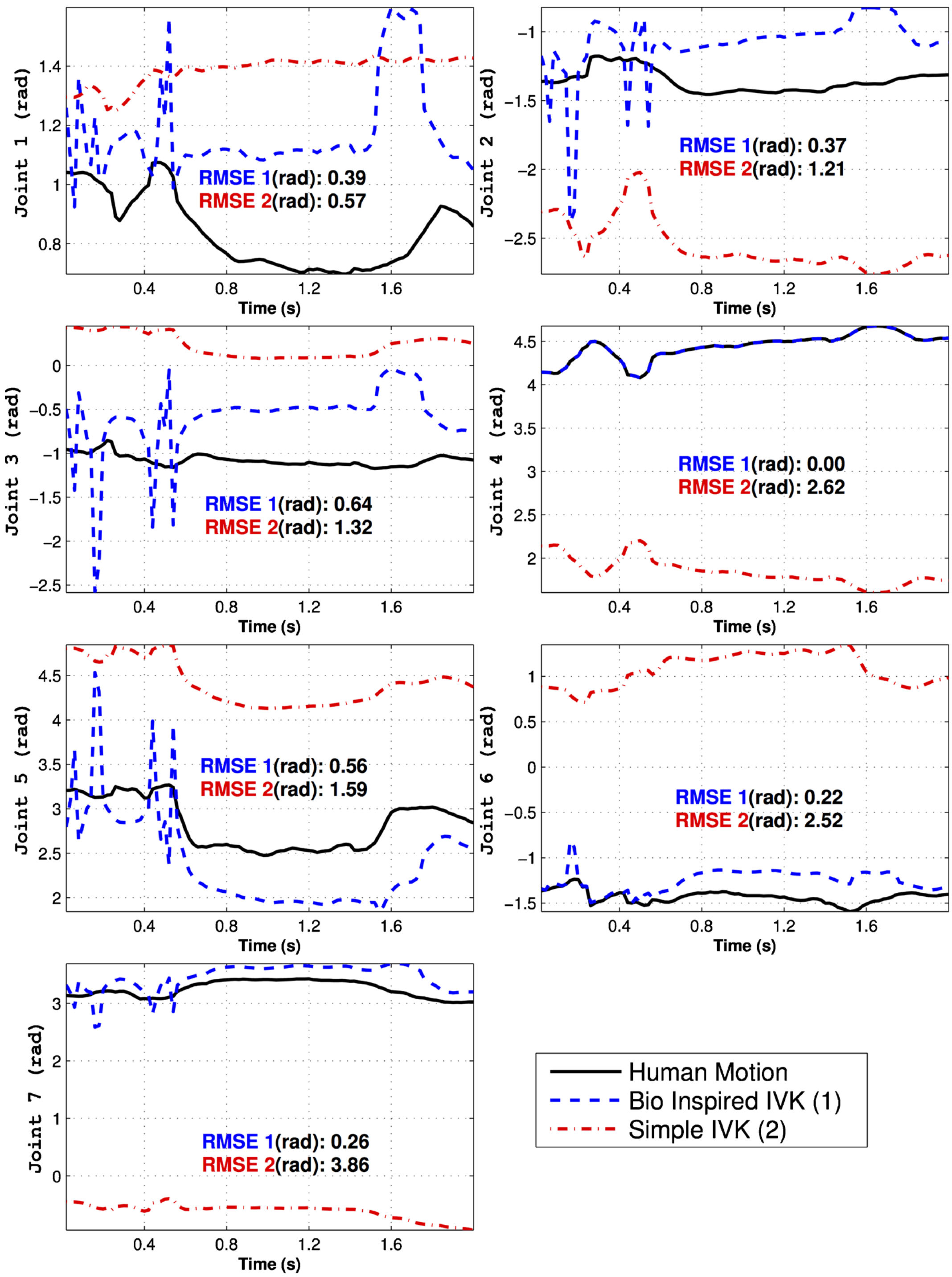

Fig. 8 Robot joints over 2 second continuous motion using the proposed method (bio-inspired controller) and the traditional pseudo-inverse Jacobian method for solving the inverse kinematics [31], compared to real motion of the replaced human arm. Root-mean-squared error (RMSE) values are reported

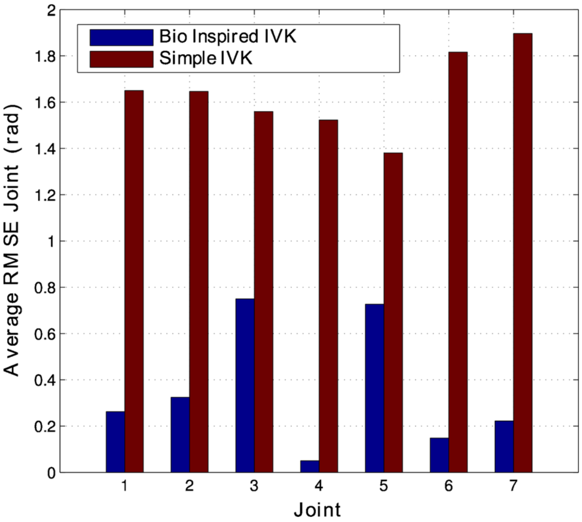

Fig. 9 Average RMSE error over entire experimental set comparing controllers to human joint data

anthropomorphic configurations, as these are characterized by the fitted PDFs. To find a representative quantification on the bio-inspired controllers success driving the arm to an anthropomorphic(high probabilistic) configuration an examination of the final joint values were tested in the probability function $P(\sigma_L)$. The distribution of the output from $P(\sigma_L)$ is shown in Fig. 10. The plot, created from 300 distinct trials,

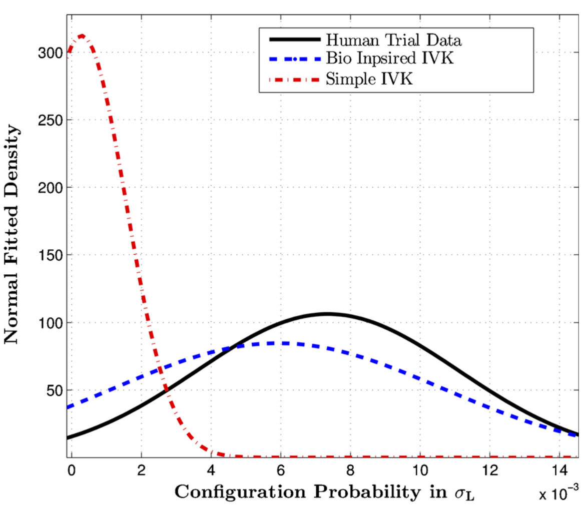

Fig. 10 Distribution for $P(\sigma_L)$ -anthropomorphic quantification- given final joint outputs of traditional and bio-inspired controllers

shows the distribution comparison between the traditional controller and the proposed one for a final configuration's anthropomorphism. Human joint configuration is also plotted to compare with the bio-inspired method. The plot shows the traditional controller ineptitude at achieving anthropomorphic configurations while the bio-inspired method's distribution is quite comparable to real human data.

The traditional inverse kinematics drives each joint without consideration of any human-like behavior: joint limits, manipulability, or even anthropomorphic intent. The controller based on the proposed method would encompass all those constraints without explicit acknowledgement. This fact can be made evident from Fig. 11 showing how, given the right arm configuration, both controllers converge on a perfect solution in end-effector pose. However, the traditional controller has solved it in a way as can be deemed non-anthropomorphic. The traditional method would drive the robot arm to collision with the model from elbow to forearm which not only results in non-anthropomorphic configuration but human apprehension from unwarranted physical human-

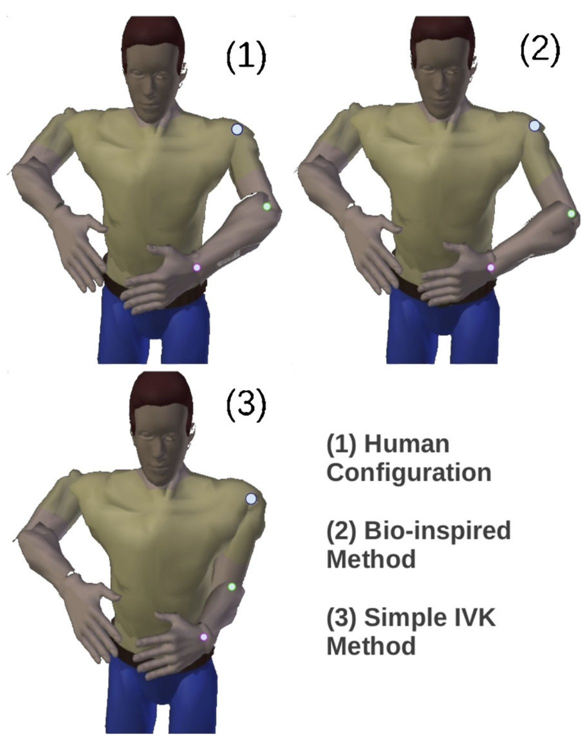

Fig. 11 Model joint comparison of inverse kinematic methods for bio-inspired and traditional controller solutions

robot contact. The bio-inspired controller drives the robot configuration to human-like posture during bi-manual tasks, which promotes more efficient interaction and collaboration between the robot and the human arm.

5 Conclusion

The future for human-robot interaction holds complicated and varied challenges in control in such an unstructured, unpredictable environment specifically in human-robot dual arm coordination. In this paper we introduced a bio-inspired controller for a robot arm that would drive the arm to anthropomorphic configurations in bi-manual human-robot collaboration tasks. As shown, the inverse kinematic controller uses real experimental data to produce human arm behavior for the robot in not only one arm (intra-arm coordination), but also mimics the inter-arm coordination of two collaborating human arms. The reduced order potential field also lends itself to arm configuration generality: allowing for a multitude of unseen tasks to still efficiently drive the inverse kinematic solution while maintaining its anthropomorphic integrity. An anthropomorphic quality metric for final arm configurations was introduced and tested for both controllers alongside real human data. The apparent downfalls of the traditional inverse kinematic methods were exemplified in comparison to the bio-inspired controller through human kinematic models during dual arm object manipulation.

References

1. Al-Gallaf, E.A.: Multi-fingered robot hand optimal task force distribution: neural inverse kinematics approach. Robot. Auton. Syst. **54**(1), 34–51 (2006)
2. Artemiadis, P.K., Kyriakopoulos, K.J.: EMG-based control of a robot arm using low-dimensional embeddings. IEEE Trans. Robot. **26**(2), 393–398 (2010)
3. Asfour, T., Dillmann, R.: Human-like motion of a humanoid robot arm based on a closed-form solution of the inverse kinematics problem. Proc. IEEE/RSJ Int. Conf. Intell. Robot. Syst. **2**, 1407–1412 (2003)
4. Bagnell, J.A., Cavalcanti, F., Cui, L.: An integrated system for autonomous robotics manipulation. In: IEEE/RSJ International Conference on Intelligent Robots and Systems, pp. 2955–2962 (2012)
5. Beetz, M., Klank, U., Kresse, I., Maldonado, A., Mösenlechner, L., Pangercic, D., Rühr, T., Tenorth, M.: Robotic roommates making pancakes. In: 11th IEEE-RAS International Conference on Humanoid Robots (2011)
6. Berg, J., Miller, S., Goldberg, K., Abbeel, P.: Gravity-Based Robotic Cloth Folding, pp. 409–424. Springer Berlin Heidelberg (2011)
7. Billard, A.: Learning human arm movements by imitation: evaluation of a biologically inspired connectionist architecture. Robot. Auton. Syst. **941**, 1–16 (2001)
8. Caggiano, V., De Santis, A., Siciliano, B., Chianese, A.: A biomimetic approach to mobility distribution for a human-like redundant arm. In: Proceedings of the IEEE/RAS-EMBS International Conference on Biomedical Robotics and Biomechatronics, pp. 393–398 (2006)
9. Cardoso de Oliveira, S.: The neuronal basis of bimanual coordination: recent neurophysiological evidence and functional models. Acta Psychol. **110**(2), 139–159 (2002)
10. Cruse, H., Wischmeyer, E., Bruser, M., Brockfeld, P., Dress, A.: On the cost functions for the control of the human arm movement. Biol. Cybern. **62**(6), 519–528 (1990)
11. Cutkosky, M.R.: On grasp choice, grasp models, and the design of hands for manufacturing tasks. IEEE Trans. Robot. Autom. **5**(3), 269–279 (1989)
12. Debaere, F., Wenderoth, N., Sunaert, S., Van Hecke, P., Swinnen, S.P.: Cerebellar and premotor function in bimanual coordination: parametric neural responses to spatiotemporal complexity and cycling frequency. Neuroimage **21**(4), 1416–1427 (2004)
13. Do, M., Azad, P., Asfour, T., Dillmann, R.: Imitation of human motion on a humanoid robot using non-linear optimization. In: 8th IEEE-RAS International Conference on Humanoid Robots, pp. 545–552 (2008)
14. Flash, T., Hogan, N.: The coordination of arm movements: an experimentally confirmed mathematical model. J. Neurosci. **5**, 1688–1703 (1985)
15. Gamage, S.S.H.U., Lasenby, J.: New least squares solutions for estimating the average centre of rotation and the axis of rotation. J. Biomech. **35**(1), 87–93 (2002)
16. Gharbi, M., Cortes, J., Simeon, T.: A sampling-based path planner for dual-arm manipulation. In: IEEE/ASME International Conference on Advanced Intelligent Mechatronics, 2008. AIM 2008, pp. 383–388 (2008)
17. Gribovskaya, E., Billard, A.: Combining dynamical systems control and programming by demonstration for teaching discrete bimanual coordination tasks to a humanoid robot. In: 3rd ACM/IEEE International Conference on Human-Robot Interaction, pp. 33–40 (2008)
18. Härtl, H.: Dextrous manipulation with multifingered robot hands including rolling and slipping of the fingertips. Robot. Auton. Syst. **14**(1), 29–53 (1995)
19. Hwang, M.J., Lee, D.Y., Chung, S.Y.: Motion Planning of bimanual robot for assembly. In: IEEE International Conference on Systems, Man and Cybernetics, 2007. ISIC, pp. 240–245 (2007)
20. Jackson, J.E.: A user's guide to principal components, vol. 587. Wiley (2005)
21. Khatib, O.: Real-time obstacle avoidance for manipulators and mobile robots. Int. J. Robot. Res. **5**(1), 90–98 (1986)
22. Kim, C., Kim, D., Oh, Y.: Solving an inverse kinematics problem for a humanoid robots imitation of human

motions using optimization. In: Proceedings of International Conference on Informatics in Control Automation and Robotics, pp. 85–92 (2005)
23. Kulic, D., Takano, W., Nakamura, Y.: Representability of human motions by factorial hidden markov models. In: Proceedings of IEEE/RSJ International Conference Intelligent Robots and Systems, pp. 2388–2393 (2007)
24. Lee, J., Sato, M., Wada, Y., Koike, Y.: Extraction of motor primitive in consideration of arm posture, movement direction and velocity using hidden markov model. In: Proceedings of the IEEE-EMBS Annual International Conference of the Engineering in Medicine and Biology Society, pp. 4385–4388 (2005)
25. McLachlan, G., Peel, D.: Finite Mixture Models. Wiley (2004)
26. Mohan, V., Morasso, P., Metta, G., Sandini, G.: A biomimetic, force-field based computational model for motion planning and bimanual coordination in humanoid robots. Auton. Robot. **27**(3), 291–307 (2009)
27. Pollard, N.S., Hodgins, J.K., Riley, M.J., Atkeson, C.G.: Adapting human motion for the control of a humanoid robot. Proc. IEEE Int. Conf. Robot. Autom. **2**, 1390–1397 (2002)
28. Potkonjak, V., Popovic, M., Lazarevic, M., Sinanovic, J.: Redundancy problem in writing: from human to anthropomorphic robot arm. IEEE Trans. Syst. Man Cybern. B **28**, 790–805 (1998)
29. Ruhr, T., Sturm, J., Pangercic, D., Beetz, M., Cremers, D.: A generalized framework for opening doors and drawers in kitchen environments. In: Proceedings IEEE International Conference on Robotics and Automation (ICRA), pp. 3852–3858 (2012)
30. Schaal, S., Kotosaka, S., Sternad, D.: Nonlinear dynamical systems as movement primitives. In: IEEE International Conference on Humanoid Robotics, pp. 1–11 (2000)
31. Sciavicco, L., Siciliano, B.: Modeling and Control of Robot Manipulators. Springer (2000)
32. Shi, J.Q., Choi, T.: Gaussian Process Regression Analysis for Functional Data. CRC Press (2011)
33. Sian, N., Sakaguchi, T., Yokoi, K., Kawai, Y.: Operating humanoid robots in human environments. In: Proceedings of the Robotics, Science & Systems Workshop on Manipulation for Human Environments, Philadelphia (2006)
34. Smith, C., Karayiannidis, Y., Nalpantidis, L., Gratal, X., Qi, P., Dimarogonas, D.V., Kragic, D.: Dual arm manipulation—a survey. Robot. Auton. Syst. **60**, 1340–1353 (2012)
35. Steffen, J., Elbrechter, C., Haschke, R., Ritter, H.: Bio-inspired motion strategies for a bimanual manipulation task. In: 2010 10th IEEE-RAS International Conference on Humanoid Robots (Humanoids), pp. 625–630 (2010)
36. Steffen, J., Pardowitz, M., Ritter, H.: Using structured UKR manifolds for motion classification and segmentation. In: IEEE/RSJ International Conference on Intelligent Robots and Systems, pp. 4785–4790 (2009)
37. Temprado, J.J., Swinnen, S.P., Carson, R.G., Tourment, A., Laurent, M.: Interaction of directional, neuromuscular and egocentric constraints on the stability of preferred bimanual coordination patterns, Human movement science (2003)
38. Inamura, T., Toshima, I., Tanie, H., Nakamura, Y.: Embodied symbol emergence based on mimesis theory. Int. J. Robot. Res. **23**(3–5), 363–377 (2004)
39. Treffner, P.J., Turvey, M.T.: Symmetry, broken symmetry, and handedness in bimanual coordination dynamics. Exp. Brain Res. **107**(3), 463–478 (1996)
40. Ude, A., Atkeson, C.G., Riley, M.: Programming full-body movements for humanoid robots by observation. Robot. Auton. Syst. **47**(2), 93–108 (2004)
41. Uno, Y., Kawato, M., Suzuki, R.: Formation and control of optimal trajectory in human multijoint arm movement. Biol. Cybern. **61**, 89–101 (1989)
42. Zacharias, F., Leidner, D., Schmidt, F., Borst, C., Hirzinger, G.: Exploiting structure in two-armed manipulation tasks for humanoid robots. In: 2010 IEEE/RSJ International Conference on Intelligent Robots and Systems (IROS), pp. 5446–5452 (2010)
43. Zhuang, J., LaConte, S., Peltier, S., Zhang, K., Hu, X.: Connectivity exploration with structural equation modeling: an fMRI study of bimanual motor coordination. Neuroimage **25**(2), 462–470 (2005)
44. Zollner, R., Asfour, T., Dillmann, R.: Programming by demonstration: dual-arm manipulation tasks for humanoid robots. In: 2004 IEEE/RSJ International Conference on Intelligent Robots and Systems, vol. 1, pp. 479–484 (2004)